Article

Nano-PAA-CuCl₂ Composite as Fenton-Like Reusable Catalyst to Enhanced Degrade Organic Pollutant MB/MO

Yang Dang [†] [ID], Yu Cheng [†], Yukun Zhou, Yifei Huang and Kaige Wang *

State Key Laboratory of Cultivation Base for Photoelectric Technology and Functional Materials, Laboratory of Optoelectronic Technology of Shaanxi Province, National Center for International Research of Photoelectric Technology & Nano-Functional Materials and Application, Institute of Photonics and Photon-Technology, Northwest University, Xi'an 710069, China; yangdang202011@163.com (Y.D.); chengyudoing@163.com (Y.C.); YuKunZhou@163.com (Y.Z.); HuangYifei1994@126.com (Y.H.)

* Correspondence: wangkg@nwu.edu.cn; Tel.: +86-1814-907-6483
† These authors contributed equally to this work.

Abstract: The treatment of organic dye contaminants in wastewaters has now becoming more imperative. Fenton-like degradation of methylene blue (MB) and methyl orange (MO) in aqueous solution was investigated by using a nanostructure that a layer of CuCl₂ nanoflake film grown on the top surface of nanoporous anodic alumina substrate (nano-PAA-CuCl₂) as catalyst. The new nano-PAA-CuCl₂ composite was fabricated with self-assembly approach, that is, a network porous structure film composed of CuCl₂ nanoflake grown on the upper surface of nanoporous anodic alumina substrate, and the physical and chemical properties are characterized systematically with the X-ray diffraction (XRD), field emission scanning electron microscope (FE-SEM), and high-resolution transmission electron microscopy (HRTEM), Energy Dispersive Spectrometer (EDS), X-ray photoelectron spectroscopy (XPS). The experimental results showed that the nano-PAA-CuCl₂ catalyst presented excellent properties for the degradation of two typical organic pollutants such as MB and MO, which were almost completely degraded with 8×10^{-4} mol/L nano-PAA-CuCl₂ catalyst after 46 min and 60 min at reaction conditions of H₂O₂ 18 mM and 23 mM, respectively. The effects of different reaction parameters such as initial pH, H₂O₂ concentration, catalyst morphology and temperature were attentively studied. And more, the stability and reusability of nano-PAA-CuCl₂ were examined. Finally, the mechanism of MB and MO degradation by the nano-PAA-CuCl₂/H₂O₂ system was proposed, based on the experimental data of the BCA and the temperature-programmed reduction (H₂-TPR) and theoretical analysis, the reaction kinetics belonged to the pseudo-first-order equation. This new nanoporous composite material and preparation technology, as well as its application in Fenton-like reaction, provide an effective alternative method with practical application significance for wastewater treatment.

Keywords: composite of nanoporous anodic alumina-CuCl₂ catalyst; Fenton-like reaction; advanced oxidation processes; organic pollutant; degradation mechanism

1. Introduction

The efficient treatment of colored sewage is still one of the main problems of textile wastewater. There are various organic pollutants contained in the textile printing and dyeing industry [1]. They are seriously harmful to the living conditions and environment since their long-lasting color, high chemical oxygen demand and non-biodegradable [2,3]. Traditional treatment methods generally cannot degrade the textile dye wastewater quickly and efficaciously. Therefore, Governments and relevant companies are passively and/or actively attracted to develop efficient and low-cost dye wastewater treatment methods [4].

Currently, more impactful decolorization technologies are anxious necessity. Various methods, e.g., physical, chemical and biological methods, have been devised for the decolorization of dye wastewater [5,6]. Among the most technologies, advanced oxidation processes (AOPs)

are regarded as effective methods for the treatment of textile pollutants [7,8]. AOPs are oxidation processes that produce hydroxyl radicals (HO•) that are effective in degrading organic contaminants due to their strong oxidizing power [9,10]. Compared with other treatment methods, AOPs have exhibited relatively high organic dye elimination efficiency and lower energy consumption under working conditions such as moderate temperature and pressure.

The Fenton oxidation process is one of the most powerful and attractive processes of AOPs [11]. Traditional Fenton reaction consisting of hydrogen peroxide (H_2O_2) and ferrous ion (Fe^{2+}, Fe(II)) has been shown to be a rapid and non-selective degradation for contaminants. In a typical homogeneous Fenton oxidation process, H_2O_2 and Fe^{2+} ions are respectively used as oxidants and catalysts, and homogeneous Fe^{2+} catalyzes H_2O_2 to produce hydroxyl radicals (HO•) for oxidizing contaminants. Fenton's equipment is simple, and the optimum conditions are verified in the pH range about 2 ~ 4. However, the Fenton reaction process has disadvantages such as high operating costs, large amounts of iron sludge, low utilization rate of H_2O_2, relatively narrow pH range of reaction, and difficulty in recovering Fe^{2+} [12,13].

Compared to Fenton reaction technology, the Fenton-like reaction process is a perfectly acceptable alternative with higher and practical activity to solve these problems by using heterogeneous catalysts [14,15]. By replacing the homogeneous Fe (II) in the Fenton process with a Fenton-like catalyst such as Cu^{2+} (Cu(II)), the defects of the Fenton reaction process can be overcome. The Fenton-like catalysts are multivalent metals such as titanium, copper, manganese, etc. These catalysts are used to activate H_2O_2 into active oxygen free radicals to degrade organic pollutants in wastewater in a Fenton-like reaction process [16,17]. About the catalysts in the Fenton-like reactions, copper-containing catalysts have significant advantages, such as low cost, rich content, and easy preparation [18,19]. Cu (II) can replace Fe (II) as a more excellent Fenton catalyst because it is suitable for a wider range of pH (3–9) and is not easy to produce impurities [20], and the reduced Cu (II)/H_2O_2 system is easier to form HO• than that of the Fe (II)/H_2O_2 system [21,22].

It has been demonstrated that the performance of Fenton-like catalysts depends partly on the surface structure and properties [23,24]. The catalytic activity will be effectively improved by increasing the specific surface area and the active sites. One of the most available ways is to make the catalysts into nanostructure materials [25]. The Fenton-like catalytic activity will be greatly enhanced by changing the copper-based catalyst into a nanoporous structure [26]. We have reported a composite that a layer of $CuCl_2$ nanoflake film grown on the top surface of nanoporus anodic alumina substrate (nano-PAA-$CuCl_2$) which was employed as catalyst of Fenton-like reaction to degrade RhB over a relatively wide pH range [27].

In this paper, the kind of composite nanostructure catalyst, that is, a network porous structure film nano-PAA-$CuCl_2$, is prepared and its physical and chemical properties are characterized systematically. The methylene blue (MB) and methyl orange (MO) are chosen as two model organic pollutants to evaluate the catalytic activity of nano-PAA-$CuCl_2$ in the Fenton-like reaction process. MB and MO are widely used and stable non-volatile industrial dyes; they belong to the most common organic pollutions. Some main reaction parameters affecting the Fenton-like reaction, e.g., the morphology of the catalyst, the initial concentration of H_2O_2, the initial pH of the reaction solution, and the reaction temperature, are systematically investigated. In addition, the stability and re-usability of the nano-PAA-$CuCl_2$ composite are examined.

2. Results and Discussion

2.1. Characteristics of Nano-PAA-CuCl₂ Composite

Figure 1 showed the image of nano-PAA-$CuCl_2$ composite. Figure 1a is a schematic diagram displaying the network of $CuCl_2$ nanoflakes grown on the top surface of the nano-PAA substrate. It can be seen that the nano-PAA template (as shown in Figure 1b) prepared by the standard two-step anodization method had uniformly distributed nanopores (~70 nm diameter) and pore interval space (~38 nm), and many discrete smaller individual

nanoflakes on the surface of the nano-PAA substrate (Figure 1c), these nanoflakes are the similar size and interconnected each other.
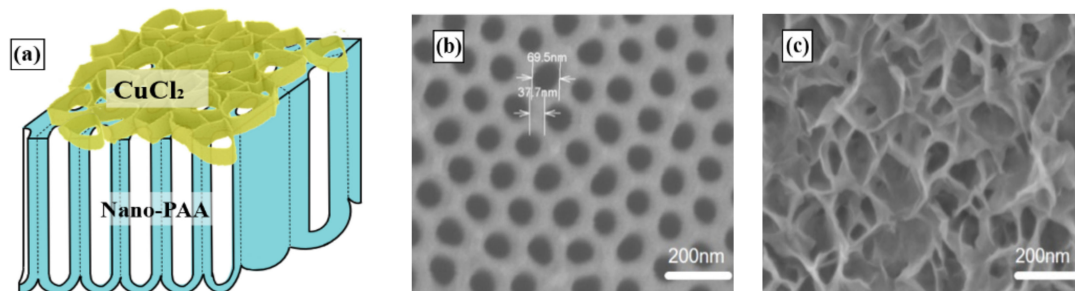
Figure 1. Image of nano-PAA-CuCl2 composite. (**a**) Diagrammatic sketch, and SEM images of nano-PAA substrate (**b**) and $CuCl_2$ nanoflakes (**c**).

To verify the elemental composition of the nano-PAA-$CuCl_2$, catalyst samples were studied by EDS and XPS as shown in Figure 2 [27].
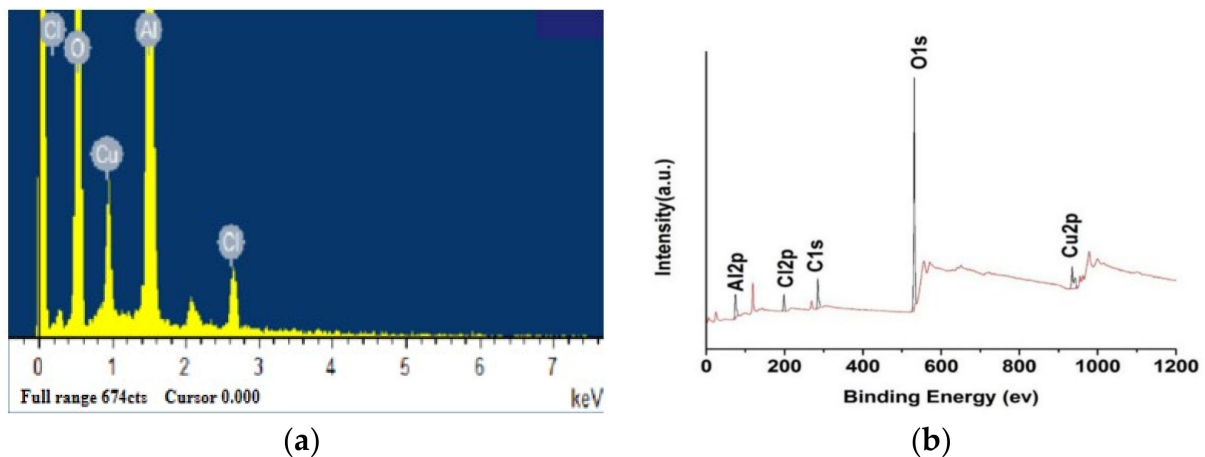
Figure 2. Elemental composition of nano-PAA-$CuCl_2$, spectrum of EDS (**a**) and XPS (**b**) [27].

As seen from Figure 2a, the catalyst contained four main elements, namely O, Al, Cu and Cl. During the measurement, the X-ray beam could directly bombard the substrate nano-PAA due to the high voltage, and therefore, the basic elements of nano-PAA, namely Al and O, were also showed. In Figure 2b, it could be seen from the peak of the XPS lines that the nano-PAA-$CuCl_2$ catalyst contained five kinds of C, O, Al, Cl and Cu elements. The C element was caused by spraying carbon on the sample surface in order to increase the conductivity. The Cu 2p XP spectrum showed a spin-orbit split bimodal, and the binding energies of Cu 2p3/2 and Cu 2p1/2 were 934.8 eV and 954.8 eV, respectively, and the difference between them was 20 eV. The characteristics of Cu XPS were exactly the same as those of Cu (II), indicating that copper existed in the form of $CuCl_2$. O 1s XPS and Al 2p XPS revealed that O 1s and Al 2p were 531.6 eV and 74.4 eV, respectively, indicating that they formed Al_2O_3 by Al-O bond.

In order to determine the spatial structure of composite nano-PAA-$CuCl_2$, the technologies of XRD and TEM were employed, and results were shown in Figure 3. The nano-PAA-$CuCl_2$ material prepared by the initial concentration of 8×10^{-4} mol/L $CuCl_2$ solution.
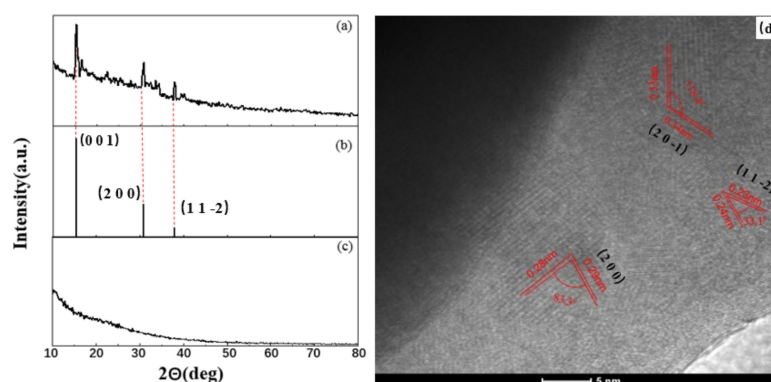
Figure 3. Space structure of composite nano-PAA-CuCl$_2$. XRD patterns of (**a**) the synthesized nano-PAA-CuCl$_2$, (**b**) standard CuCl$_2$ spectrum, (**c**) substrate nano-PAA film, and (**d**) HR-TEM micrograph.

It could be seen from Figure 3a, three peaks were detected at $2\theta = 15.36, 30.64, 37.88$. These spectra are the peaks of CuCl$_2$ as shown in Figure 3b, comparing with the JCPDS file data (CuCl$_2$, JCPDS no. 35-0690). In the spectrum as shown in Figure 3a, there was not found the peak of Al$_2$O$_3$, as a comparison, Figure 3c displayed the XRD characterization of the subtract nano-PAA film. Figure 3d was HRTEM micrograph of the nano-PAA-CuCl$_2$ catalyst. It could be observed that the lattice edges of the material are transparent, which indicates that the top layer CuCl$_2$ had a crystal structure. As shown by those red lines in Figure 3d, there were several different interplanar spacings and angles, which indicated that the top lay of nano-PAA-CuCl$_2$ film had different crystal grains and different crystal phases, that is, it was a polycrystalline structure. Comparing with Figure 3a, the spacing of each lattice fringe corresponded to the certain XRD result, that is, the 0.34 nm spacing corresponded to the $(2\ 0\ -1)$ crystal orientation, the 0.24 nm spacing corresponded to the $(1\ 1\ -2)$ crystal orientation, and the 0.28 nm spacing corresponded to the $(2\ 0\ 0)$ crystal orientation. The competition between different phases and different growth directions led to the formation of CuCl$_2$ nanoflakes, and the nanoflakes grew in different directions to form an overall nanoporous structure.

2.2. Degradation of MB and MO Solution

2.2.1. Degradation Processes

Different treatments on the catalytic degradation of MB and MO were studied with the following comparison experiments: nano-PAA-CuCl$_2$, H$_2$O$_2$, or solid-state catalyst/H$_2$O$_2$ system. As a contrast, solid-state catalysts included two types, CuCl$_2$ particles and nano-PAA-CuCl$_2$ composite. All experiments were performed at room temperature and the initial solution pH = 3. Figure 4 displayed the degradation effects of different treatment processes.

For comparative studies and analysis, a set of blank experiments were performed to evaluate the degradation ability of the H$_2$O$_2$ or nano-PAA-CuCl$_2$ alone on the MB or MO in aqueous solution.

From Figure 4a,c, it can be clearly found without a solid-state catalyst, H$_2$O$_2$ only cause slight degradation of MB or MO, which might be attributed to its weaker ability to decompose HO•, and therefore cannot effectively degrade MB or MO [28,29]. Similarly, in the absence of H$_2$O$_2$, there was alone nano-PAA-CuCl$_2$ composite or CuCl$_2$ particles in the dye solution, the MB or MO solution also had no obvious degradation, which was attributed to the weak adsorption capacity of the catalyst itself. It is obvious that the degradation of MB or MO solutions was almost negligible without the solid-state catalyst/H$_2$O$_2$ system.
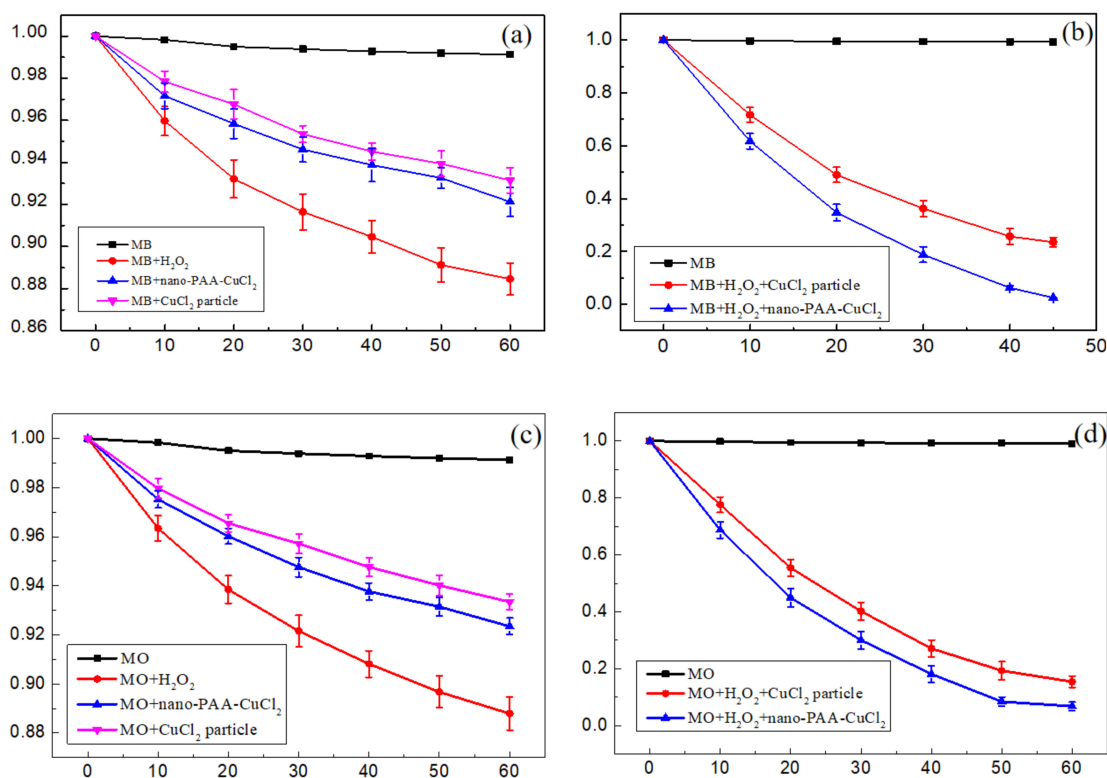
Figure 4. Degradation of MB and MO solution treated with different processes: (**a**) H_2O_2, nano-PAA-CuCl$_2$ composite and CuCl$_2$ particle in MB solution, (**b**) CuCl$_2$ particle/H_2O_2 and nano-PAA-CuCl$_2$ composite/H_2O_2 in MB solution, (**c**) H_2O_2, nano-PAA-CuCl$_2$ composite and CuCl$_2$ particle in MO solution, (**d**) CuCl$_2$ particle/H_2O_2 and nano-PAA-CuCl$_2$ composite/H_2O_2 in MO solution.

Figure 4b,d showed the catalytic activities of nano-PAA-CuCl$_2$ composite and CuCl$_2$ particles in the presence of H_2O_2, respectively. It could be found that the degradation of the MB or MO solutions had been significantly promoted by the nano-PAA-CuCl$_2$/H_2O_2 system or the CuCl$_2$ particles/H_2O_2 system. However, it should be noted that the degradation levels of MB or MO solutions with the CuCl$_2$ particle catalysts were lower than that of using the nanoPAA-CuCl$_2$ composite catalysts. These results indicated that the catalytic activities of the nano-PAA-CuCl$_2$ composites were better than that of the CuCl$_2$ particles.

Figure 5 displayed a series of photographs of MO and MB solutions that were catalytically degraded in real-time by the nano-PAA-CuCl$_2$ composite/H_2O_2 system. It can be clearly seen that the color of the analyzed solutions changed from turbidity to discoloration, and became transparent within 60 min.

2.2.2. Influencing Factors about Degradation

The main factors affecting the degradation of organic pollutants MB and MO by the catalyst nano-PAA-CuCl$_2$ composite in the Fenton-like reaction process have been systematically studied and analyzed.

Effect of Spatial Structure of Nano-PAA-CuCl$_2$ Composite

The catalytic performance of the Fenton-like reaction is affected greatly by the catalyst spatial structure and surface morphology, and the adsorption and decolorization rate of dye wastewater depend partly on the catalyst structure properties [27].

In order to systematically study the effect of catalyst structure and morphology on the degradation of MB or MO solution, a series of nano-PAA-CuCl$_2$ catalysts with different morphologies and spatial structures were prepared according to the different initial concentration of CuCl$_2$ solutions, as shown in Figure 6. Decolorization reactions were carried

out with these different composite nano-PAA-CuCl$_2$ catalysts, and Figure 7 displayed the corresponding degradation properties.
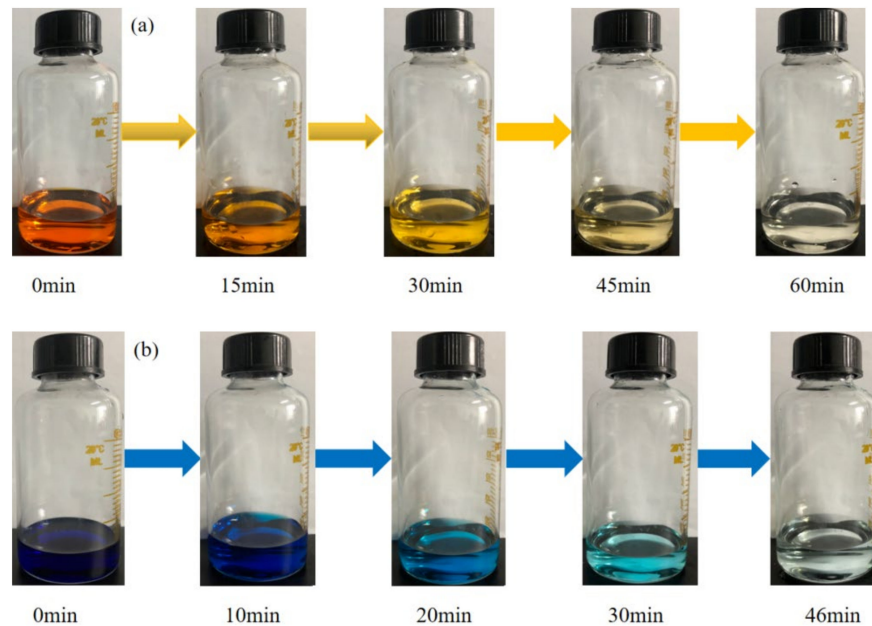
Figure 5. Photographs of (**a**) MO and (**b**)MB solutions with color changed form heavy to clear catalytically degraded with nano-PAA-CuCl2 composite/H$_2$O$_2$ system.
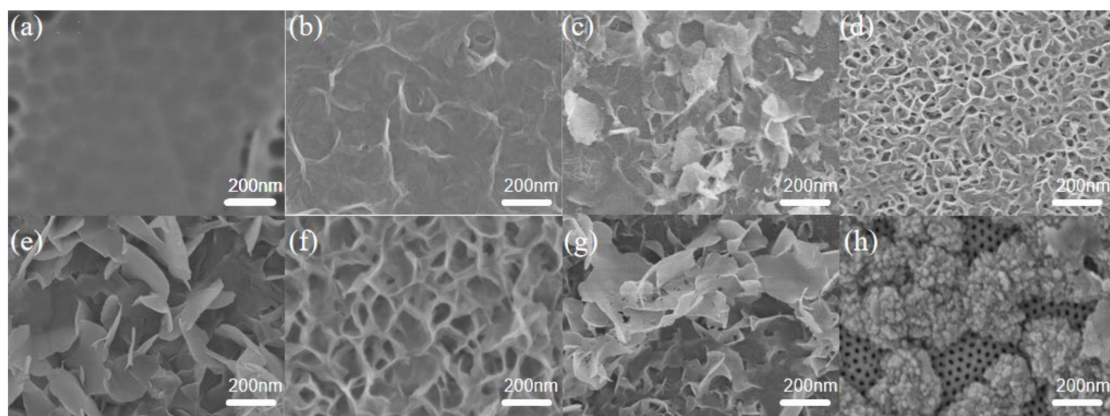
Figure 6. SEM images of nano-PAA-CuCl$_2$ composite, CuCl$_2$ nanoflakes grown on the top surface of nano-PAA substrates with different initial concentrations of CuCl$_2$ solution. (**a**) 1×10^{-4} mol/L, (**b**) 2×10^{-4} mol/L, (**c**) 3.5×10^{-4} mol/L, (**d**) 5×10^{-4} mol/L, (**e**) 6×10^{-4} mol/L, (**f**) 8×10^{-4} mol/L, (**g**) 9.5×10^{-4} mol/L, and (**h**) 1.5×10^{-3} mol/L.

As shown in Figure 6a, when the initial concentration of the CuCl$_2$ solution was 1×10^{-4} mol/L, a large-area nanopore could be clearly seen on the top nano-PAA film, and only a little amount of sparse CuCl$_2$ material was covered on the surface. In Figure 6b, the catalyst was prepared by using initial concentration of 2×10^{-4} mol/L CuCl$_2$ solution. It was observed that large-area flocculation structures were formed and covered on the top surface of the nano-PAA film, but they were not interconnected to form independent nanoflakes. Figure 6c showed that when the concentration continued to increase to 3.5×10^{-4} mol/L, a layer of CuCl$_2$ film composed of independent nanoflakes had been formed, and the nanoflakes were independent of each other. As shown in Figure 6d, when the initial concentration of CuCl$_2$ solution was 5×10^{-4} mol/L, the nano-CuCl$_2$ film was uniform and covered the top surface of nano-PAA substrate, and the nanoflakes had gradually connected each other, a porous-like film had clearly formed. In Figure 6e, it could be found that there were many independent

nanoflakes, although the shape and the size of these nanoflakes were different and the spatial structure was not uniform, when using an initial 6×10^{-4} mol/L CuCl$_2$ solution. Figure 6f showed that the composite nano-PAA-CuCl$_2$ when the initial CuCl$_2$ solution concentration was increased to 8×10^{-4} mol/L. It could be seen there were a great deal of nanoflakes with uniform structural size on the top surface of the nano-PAA substrate, these nanoflakes were combined to form a porous structure, and completely covered the upper surface nano-PAA film. However, when the initial concentration of the CuCl$_2$ solution was increased to 9×10^{-4} mol/L, the structure of the nano-film gradually became messy again, as shown in Figure 6g, and the shape and size of nanoflakes were different and not connected to each other. When the initial CuCl$_2$ solution was 1.5×10^{-3} mol/L, the structure and morphology of the nano-PAA-CuCl$_2$ composite was shown in Figure 6h, it could be found that the nano-particle structures were stacked on the upper surface of the nano-PAA substrate.
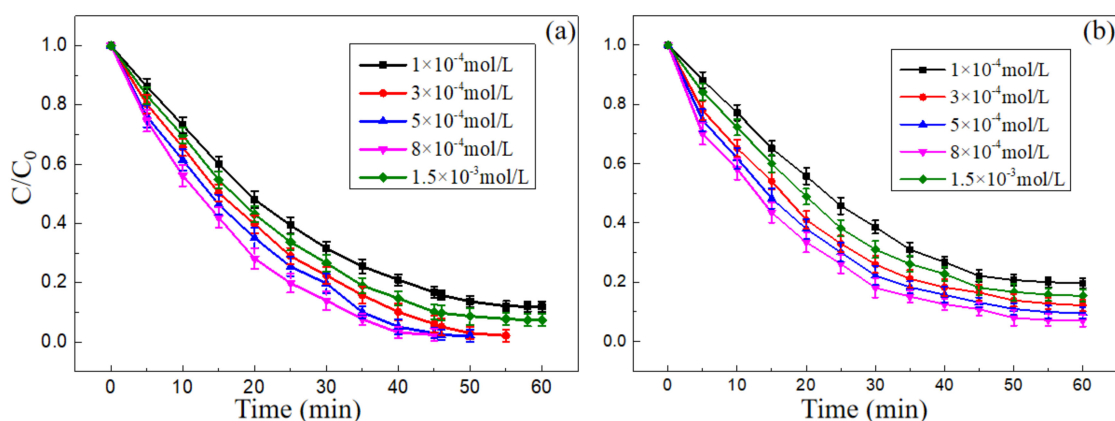
Figure 7. Effect of spatial structure of nano-PAA-CuCl$_2$ catalyst on the degradation, (**a**) MB and (**b**) MO. Experimental conditions: initial H$_2$O$_2$ concentration 18 mM for MB and 23 mM for MO, initial pH value of 3, 30 °C.

The decolorization performance of MB and MO reduced by the composite nano-PAA-CuCl$_2$ catalyst with different morphologies was investigated systematically. Figure 7 displayed the effect of catalytic spatial structure and morphology on degradation. As shown in Figure 7, the optimal degradation rates were achieved when the composite nano-PAA-CuCl$_2$ catalysts were used as shown in Figure 6d,f. The main reasons probably due to their large number of nanoflakes with uniform structures and sizes, and the large contact area with the solution by combined these nanoflakes to form a porous structure. These porous structures increased the contact surface area, thus increasing the adsorption of the reactants and providing more active sites for H$_2$O$_2$ activation. In the following experiments, the composite nano-PAA-CuCl$_2$ catalysts as shown in Figure 6f were chosen.

Effect of pH

The Fenton reaction could usually achieve a better result under acidic conditions. The effect of initial pH of solution on the degradation of MB and MO was studied in a wide pH range (2–12) as shown in Figure 8. The experimental conditions were as follows: nano-PAA-CuCl2 composite catalyst was synthesized with 8×10^{-4} mol/L CuCl$_2$ solution at 30 °C; the initial H$_2$O$_2$ concentrations for MB and MO were 18 mM and 23 mM, respectively. It can be found from Figure 8, the pH value had a decisive influence on the Fenton-like reaction to degrade MB and MO.
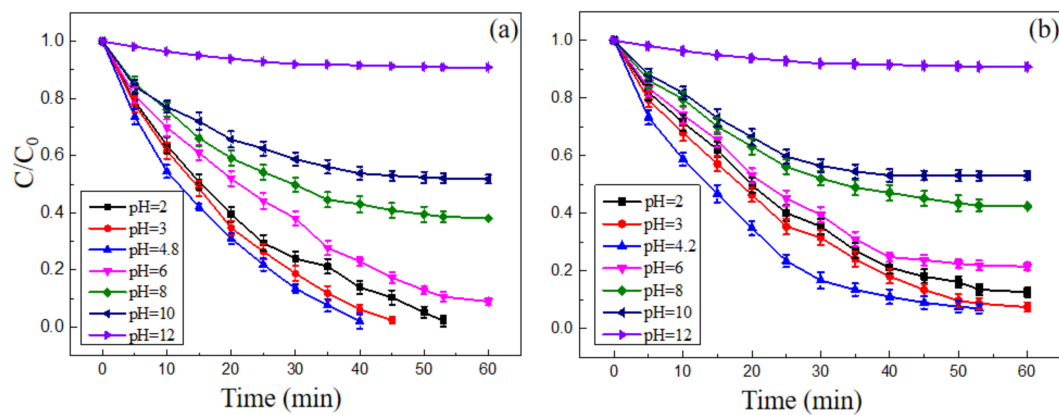
Figure 8. Effect of solution initial pH value on the degradation of (**a**) MB and (**b**) MO. Experimental conditions: initial H_2O_2 concentration 18 mM for MB and 23 mM for MO, the composite catalyst synthesized with 8×10^{-4} mol/L $CuCl_2$ solution at 30 °C.

As shown in Figure 8a, when the pH was 4.8, MB could be almost completely degraded in a relatively short period of time. Meanwhile, when pH was 2~4.8, MB could also be almost completely degraded rapidly. However, as the pH gradually increased to 12, the degradation rates of MB gradually decreased. Similarly, Figure 8b showed that the pH = 4.2 was the optimum value for degrading the MO pollutant solution. When the pH was 2~4.2, the MO solution could still be degraded efficiently. When the pH was gradually increased, the degradation rate of MO decreased, particularly, when the pH reached 12, the degradation of MO became negligible. These results could be attributed to the fact that the H_2O_2 was unstable in alkaline solutions and easily decomposed into oxygen and water, as expressed in Equation (1):

$$H_2O_2 \xrightarrow{pH=12} H_2O + O_2 \tag{1}$$

From Figure 8, it can be observed that a suitable initial pH range for the solution was 2~8 to degrade the MB and MO, and when the pH was 4.8 or 4.2, the MB or MO solution had the best degradation effect, respectively. That is to say, the composite nano-PAA-$CuCl_2$ catalyst could perform an effective redox reaction over a wider pH range.

Effect of H_2O_2 Concentration

The concentration of H_2O_2 had a great influence on the results of the Fenton-like reaction. The oxidations of MB and MO with 8×10^{-4} mol/L nano-PAA-$CuCl_2$ composite and different H_2O_2 concentration at pH 3.0 were investigated as shown in Figure 9.
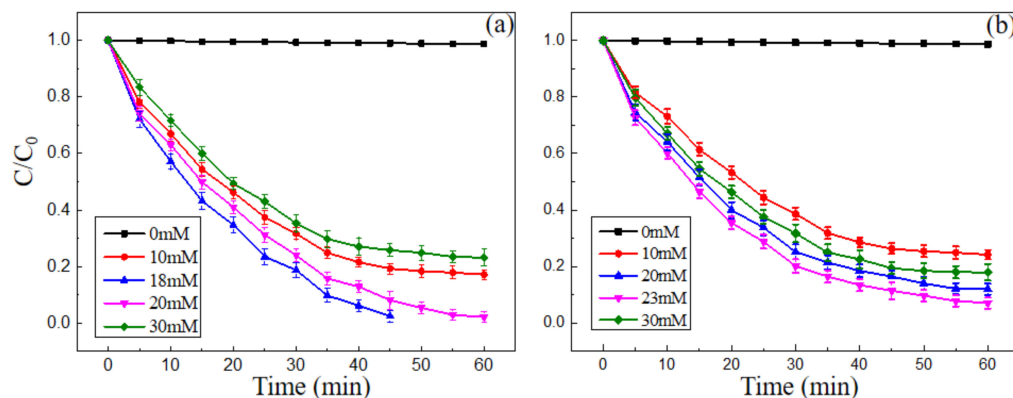
Figure 9. Effect of initial H_2O_2 concentration on the degradation of (**a**) MB and (**b**) MO solution. Experimental conditions: initial pH value of 3, catalyst synthesized with 8×10^{-4} mol/L $CuCl_2$ solution, 30 °C.

In the Fenton-like reaction process, the degradation of MB or MO solution was dominantly caused by the hydroxyl (HO•) generated by the decomposition of H_2O_2, which could be expressed as Equations (2) and (3) [30].

$$Cu(II) + H_2O_2 \rightarrow Cu(I) + HO_2 + H^+ \tag{2}$$

$$Cu(I) + H_2O_2 \rightarrow Cu(II) + OH^- + HO\bullet \tag{3}$$
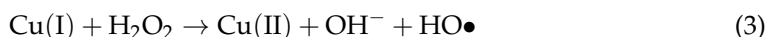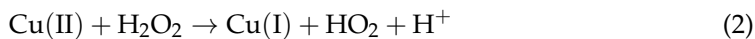
Figure 9 displayed the degradation rates of MB and MO when the initial concentration of H_2O_2 was varied from 0 to 30 mM. The experimental conditions were initial pH of 3, nano-PAA-CuCl$_2$ catalyst concentration of 8×10^{-4} mol/L and 30 °C. It could be seen that when the initial concentration of H_2O_2 was increased from 10 mM to 18 mM, the MB degradation rate increased from 80.9% to 97.1% at 46 min (Figure 9a), and the MO degradation rate increased from 75.8% to 92.7% at 60 min when the initial concentration of H_2O_2 was increased from 10 mM to 23 mM (Figure 9b). However, it should be noted that when the H_2O_2 concentration was further increased to 30 mM (data not shown), both the degradation rates of MB and MO did not increase but decreased. Therefore, in the following experiments, the 18 mM or the 23 mM was selected as the H_2O_2 concentration to effectively degrade MB or MO.

Effect of Temperature

In general, the kinetic constant has an exponential relationship with temperature [28], so the chemical reaction accelerates as the temperature increases. In the Fenton-like system, the reaction processes are always more complicated, there are forward reactions, but also reverse reactions. The increase of temperature can not only accelerate the progress of a forward reaction, but also enhance a reverse reaction. In addition, high temperature has severe limitations in practical applications. Thus, the effect of temperature on Fenton-like reaction treatment of wastewater is more complicated and need to be further investigated seriously.

Figure 10 showed the degradation rate of MB and MO at different temperatures, H_2O_2 concentration was 18 mM or 23 mM, composite nano-PAA-CuCl$_2$ synthesized with 8×10^{-4} mol/L CuCl$_2$ solution and initial pH was 3.
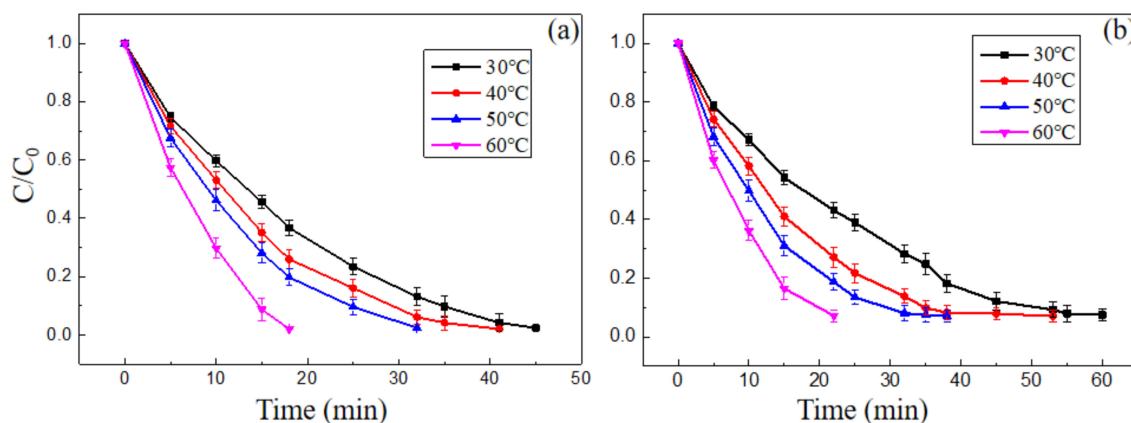
Figure 10. Effect of temperature on the degradation of (**a**) MB and (**b**) MO. Experimental conditions: initial H_2O_2 concentration 18 mM for MB and 23 mM for MO, initial pH value was 3, composite catalyst synthesized with 8×10^{-4} mol/L CuCl$_2$ solution.

As shown in Figure 10, the decolorization reaction were proceeded at different temperatures ranged from 30 °C to 60 °C. During the reaction process, no higher temperatures were used because excessively high temperatures were more limited in practical applications and might cause the decomposition of H_2O_2 into O_2 and HO_2, which would weaken the efficiency of the oxidation reaction [31].

In Figure 10a, it can be found that the MB solution was completely degraded after 46 min, 41 min, 32 min and 18 min at temperatures of 30 °C, 40 °C, 50 °C and 60 °C, respectively. That is, the degradation rate was increased as the working temperature increased. Similarly, as the temperature increased, the degradation rate of the MO solution also increased as shown in Figure 10b. A more reasonable explanation for the above results is that as the working temperature increased, both the amount and generation rate of HO• produced by the nano-PAA-CuCl$_2$/H$_2$O$_2$ system increased, so the decolorization process was completed quickly. The degradation rate of MB or MO solution quantitatively increased with the increase of the kinetic rate, complying with the Arrhenius equation, i.e., an exponential law of reaction rate. Therefore, the working temperature was appropriately raised, the catalytic activity of nano-PAA-CuCl$_2$/H$_2$O$_2$ system would be greatly improved, as a result, the degradation time was greatly reduced.

2.3. Reusability of Nano-PAA-CuCl$_2$ Catalyst

Reusability is one of the most important factors for evaluating the performance of catalyst in practical applications of Fenton-like reactions. A series of experiments should be performed in order to evaluate the reusing possibility of the prepared catalyst. The reusability of the nano-PAA-CuCl$_2$ composite was examined by repeating the catalytic reaction several times under the same working conditions. Figure 11 showed the degradation rates of the nano-PAA-CuCl$_2$ catalyst for MB solution (Figure 11a) and MO solution (Figure 11b) during cyclic experiments. In the experiments, the nano-PAA-CuCl$_2$ composite catalyst was firstly taken out from the solution by filtration after each degradation process completed, and then washed and dried before used in the next cycle experiment. Experimental data as shown in Figure 11 clearly indicated the nano-PAA-CuCl$_2$ composite catalyst had excellent reusability.
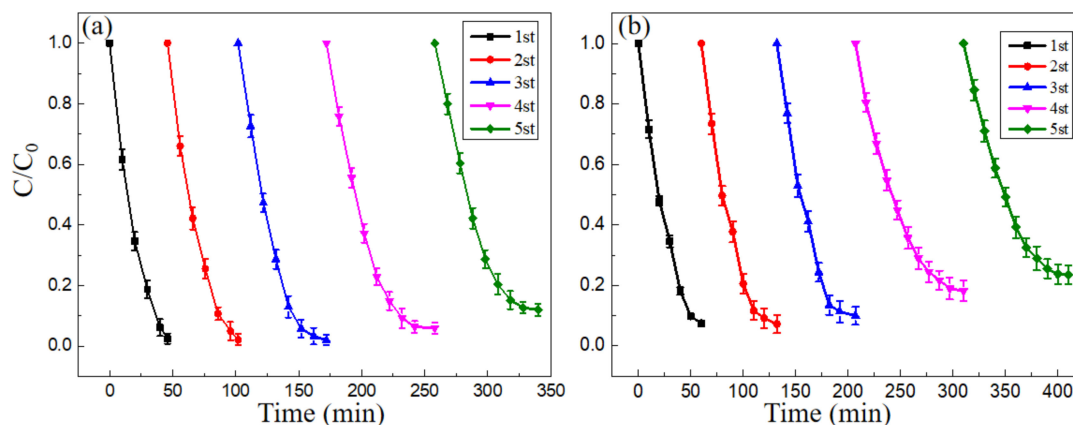
Figure 11. Reusability of nano-PAA-CuCl$_2$ composite for Fenton-like reaction with MB (**a**) and MO (**b**). Reaction conditions: initial H$_2$O$_2$ concentration 18 mM for MB and 23 mM for MO, initial pH value 3, catalyst synthesized with 8×10^{-4} mol/L CuCl$_2$ solution, 30 °C.

From Figure 11, it can be found that the new catalyst could be recycled in the Fenton-like reaction processes to degrade the organic pollutants of MB and MO. Specifically, the MB solutions could be completely degraded (100%) for three times, and the MO solutions could be almost completely done for two times (~95%). Moreover, when the composite nano-PAA-CuCl$_2$ catalyst was repeatedly used, even for the fifth time in a row, it still maintained a high degradation rate (about 90% for MB and ~80% for MO), although the degradation time increased.

2.4. Degradation Mechanism of Nano-PAA-CuCl$_2$/H$_2$O$_2$ System

2.4.1. Detecting Cu$^+$ Ions (Cu (I))

In the Fenton-like reaction, the metal ion-containing catalyst generally has two valence states that inter converted into each other and can react with H$_2$O$_2$ to promote a strong oxidative radical which will degrade organic pollutants.

In order to accurately judge and understand the chemical reaction that occurred during the degradation of pollutants (MB or MO) caused by the nano-PAA-CuCl$_2$ composite, the bicinchoninic acid (BCA) method was used to monitor the change of Cu(I) during the reaction process, the absorption spectra were shown in Figure 12.
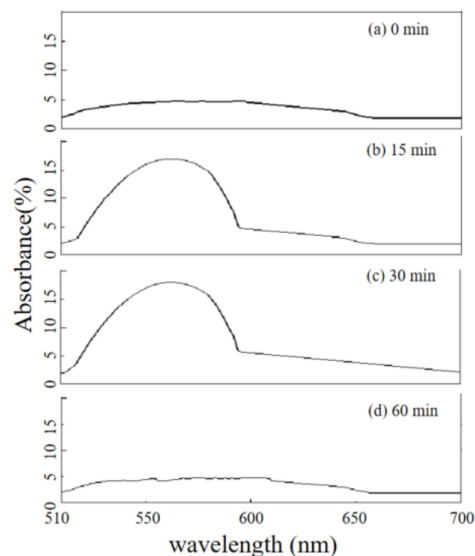
Figure 12. Absorption spectra of the solution of BCA and MO recorded every 15 min to determine Cu (I) ions. (**a**) 0 min, (**b**) 15 min, (**c**) 30 min, and (**d**) 60 min.

It is well known that BCA can form a complex with Cu(I), and a trace amount of Cu(I) ions can be determined by measuring complex absorbance at 562 nm [32]. During experiments, about 10 mL H$_2$O$_2$ (18 mM) solution and MO solution was added to a dedicated beaker, and the nano-PAA-CuCl$_2$ composite was added to start up the redox reaction. This solution was used as the blank reagent. Then an appropriate amount of BCA reagent was added into the beaker. The color and absorption spectra of the solution were monitored with the spectrophotometer, and the UV-*vis* absorption spectra were recorded every 15 min to determine whether Cu (I) ions being contained. Form Figure 13, it can be observed clearly that at the beginning of the experiment (Figure 12a), there was no significant enhance in absorbance around 562 nm, indicating that the solution did not contain Cu (I) ions, thus the Fenton-like reaction did not occur. When the reaction continued to 15 min (Figure 12b), a significant increase in absorbance near 562 nm was detected, indicating that Cu (I) ions were present in the solution and a Fenton-like reaction had been occurred. Keeping the same conditions until 30 min (Figure 12c), Cu (I) ions could still be detected, revealing the Fenton-like reaction was still proceeding. When the reaction was lasted for 60 min (Figure 12d), Cu (I) ion was almost no longer detected in the solution, indicated that the Fenton-like reaction had been completed.

The redox activity can be analyzed with the H$_2$-TPR method. Figure 13 displayed the H$_2$-TPR profiles of nano-PAA-CuCl$_2$ composite. For comparison, the H$_2$-TPR curve of CuCl$_2$ particle was also measured. In general, in a Fenton-like reaction system, metal ions were converted between different chemical valence states, such as the mutual transformation between Cu(II) and Cu(I) [33].
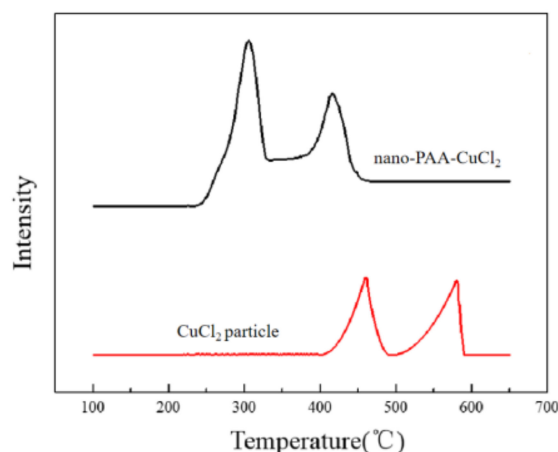
Figure 13. H_2-TPR profiles of nano-PAA-$CuCl_2$ composite and $CuCl_2$ particle.

As shown in Figure 13, there were two peaks at 310 °C and 415 °C, which indicated a two-step reduction of the nano-PAA-$CuCl_2$ composite catalyst. The reduction peak at 310 °C corresponded to the reduction of the Cu (II) to the Cu (I), and the reduction peak at 415 °C corresponded to the Cu (I) reduced to the Cu (0). It could be seen in Figure 13 that the reduction peaks of $CuCl_2$ particles were also two peaks, i.e., 460 °C and 580 °C, Rouco has reported the similar result [34]. Compared with the nano-PAA-$CuCl_2$ composite, the position and shape of reduction peaks in the H_2-TPR curve of $CuCl_2$ particles were different. These H_2-TPR curves indicated that the nano-PAA-$CuCl_2$ catalyst had higher redox activity.

2.4.2. Catalytic Mechanism

About the Fenton catalytic degradation of MB or MO with nano-PAA-$CuCl_2$/H_2O_2 system, copper ions reacted with H_2O_2 to catalyze the production of (HO•) [35]. During the heterogeneous Fenton-like catalytic degradation, the interaction process among the nano-PAA-$CuCl_2$, H_2O_2 and MB or MO was schematically illustrated in Figure 12. During the Fenton-like reaction, the HO• produced by the interaction between H_2O_2 and catalyst degraded the organic dye contaminants into CO_2 and H_2O.

As shown in Figure 14, the decolorization reaction had two main effective processes, namely the ability to effectively degrade and recycle. The reaction process could be described as the following equations:

$$Cu(II) + H_2O_2 \rightarrow CuOOH^+ + H^+ \tag{4}$$

$$CuOOH^+ \rightarrow Cu(I) + O_2\cdot + H^+ \tag{5}$$

$$Cu(II) + HO_2\cdot \rightarrow Cu(I) + O_2 + H^+ \tag{6}$$

$$Cu(II) + O_2\cdot \rightarrow Cu(I) + O_2 \tag{7}$$
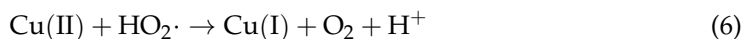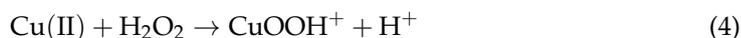
During the degradation process, Cu (I) reacted with H_2O_2 to form HO• (Equation (3)). After the nano-PAA-$CuCl_2$ catalyst was mixed with H_2O_2 in the dye solution, a hydroperoxide was first formed by a reduction reaction of Cu (II) (Equation (4)). Subsequently, $CuOOH^+$ was decomposed into Cu (I) and superoxide anion (O_2•), such as Equation (5) [30]. At the same time, Cu (II) reacted with the hydroperoxide radicals. (HO_2•) and superoxide radical anion (O_2•) produced in Equations (4) and (5) to form Cu (I) (Equations (6) and (7)). In this type of Fenton reaction, HO_2• and O_2• were important intermediates for the conversion of Cu (II) to Cu (I) [36]. HO_2• and O_2• could also played a weak role in the degradation of MB/MO solution, but the reactivity of HO_2• and O_2• was much lower than that of HO•. Finally, Cu (II) could also be produced during the reaction of Cu (I) with H_2O_2

to form HO•, and a cyclic reaction was formed. Therefore, the Cu (II)/H_2O_2 system and the Cu (I)/H_2O_2 system construct a catalytic cycle [27].
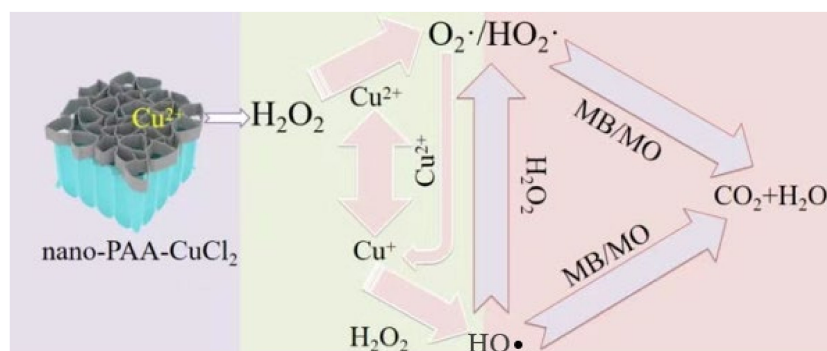
Figure 14. Schematic diagram of the mechanism of catalytic degradation of MB/MO by nano-PAA-CuCl$_2$/H$_2$O$_2$ system.

It is evident from all the above that the nano-PAA-CuCl$_2$/H$_2$O$_2$ system exhibited high activity and stability during the degradation of MB or MO, mainly due to its large specific surface area and the coexistence of Cu (II)/Cu (I) during the reaction. The interaction of H$_2$O$_2$ with the surface of the copper dichloride caused the formed beta-HO• radicals to attack the adsorbent or contaminants in the aqueous phase. That was to say, the high efficiency of the Fenton catalytic reaction of the nano-PAA-CuCl$_2$/H$_2$O$_2$ system might be the result of a combination of physical adsorption and chemical reaction. The nano-PAA-CuCl$_2$ composite catalyst had many micropores/nanopores, this distinctive spatial structure ensured that it could physically adsorb a large amount of organic dye contaminants.

The Fenton-like reaction kinetics could be described as: $C/C_0 = \exp(-kt)$ with the advancement of the catalytic degradation of MB of MO by the nano-PAA-CuCl$_2$/H$_2$O$_2$ system. Where k was the observed first-order reaction rate constant (min^{-1}), t was the reaction time (min), C_0 was the initial concentration of MB or MO (mg/L), and C was the concentration (mg/L) of MB or MO. Figure 14 showed the relationship between $-\ln(C/C_0)$ versus time t.

The order of reaction with respect to MB (Figure 15a) or MO (Figure 15b) could be determined with the regression analysis. It could be seen from Figure 15 that the $-\ln(C/C_0)$ $- t$ was highly consistent with $y = kx + b$, so these Fenton-like reactions conformed to the pseudo-first-order kinetic equation, the correlation coefficient R^2 was close to 0.98. In fact, all the catalytic degradation of MB or MO with nano-PAA-CuCl$_2$/H$_2$O$_2$ system, the reaction kinetics can be described as the Equation: $C/C_0 = \exp(-kt)$, the curves of C/C_0 with time as shown in Figure 7 to Figure 11 are all well consistent with the equation, i.e., the kinetics of oxidation degradation of MB or MO followed the pseudo-first-order equation.
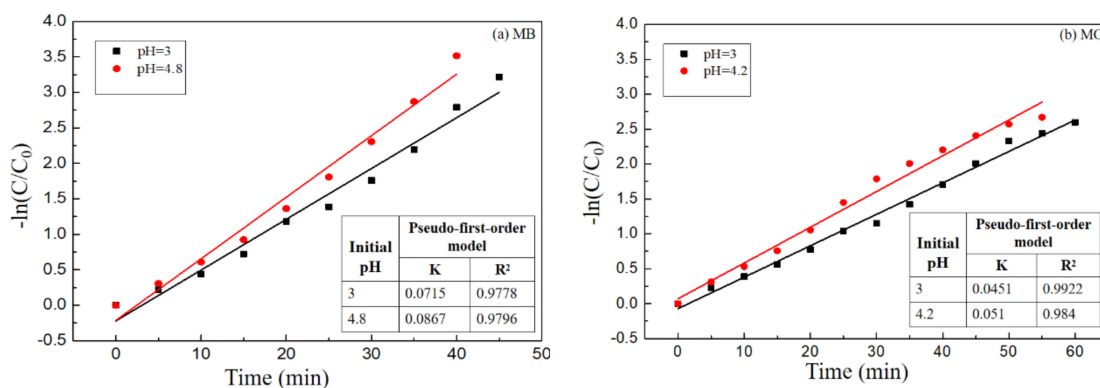
Figure 15. Oxidation kinetic of (**a**) MB and (**b**) MO degradation according with the pseudo-first-order equation relationship.

3. Materials and Methods

3.1. Materials

Copper dichloride ($CuCl_2$, Shengao Chemical Reagent Co., Ltd., Xi'an, China), Hydrogen peroxide (H_2O_2, 30%, *v/v*, Damao Chemical Reagent Factory, China), Oxalic acid ($C_2H_2O_4$, Tianli Chemical Reagent Co., Ltd., Tianjin, China), Methylene blue and methyl orange (MB and MO, Sigma-Aldrich Shanghai Trading Co., Ltd., Shanghai, China), Bicinchoninic acid (BCA, Aladdin Industrial Corporation, Shanghai, China), are all chemically pure. The metal aluminum films (99.999%, Beijing Non-ferrous Metal Co., Ltd., Beijing, China) are super-purity. All experimental solutions are prepared with deionized (DI) water.

3.2. Preparation of Nano-PAA-CuCl₂ Composites

The preparation of the composite nano-PAA-$CuCl_2$ can be described simply as the following two steps [37]. Firstly, the substrate nanoporous anodic alumina (nano-PAA) was synthesized with the standard two-step anodization method [38]. In this process, 0.3 mol/L oxalic acid was used as the oxidizing electrolyte, oxidation voltage was 40 V, the time of the first and second oxidation was 1 h and 2 h respectively, the time of removing primary membrane was 1 h, the time of widening pore was 1.5 h, and the back aluminum layer was removed by the $CuCl_2$ solution. Secondly, a $CuCl_2$ nanoflake film was grown on the upper surface of the nano-PAA substrate by the self-assembled method [39], i.e., a certain concentration of $CuCl_2$ solution (ranging from 1×10^{-4} mol/L to 1.5×10^{-3} mol/L) was dropped onto the surface of the nano-PAA substrate until the inside pores of nano-PAA film were filled, then the $CuCl_2$ nanoflake film grew up with the self-assembled method at room temperature for more than 7 days in a closed clean environment.

3.3. Sample Characterizing

The morphologies of nano-PAA and nano-PAA-$CuCl_2$ were all characterized by a field emission scanning electron microscope (FE-SEM, Hitachi-SU8010, Hitachi Works, Ltd., Tokyo, Japan) and the spatial structure with a high-resolution transmission electron microscopy (HRTEM Tecnai G2 F20, FEI, Hillsboro, OR, USA). Energy-dispersive spectrometer (EDS, JEM-2100, Japan Electronics Corporation, Tokyo, Japan) was employed to detect the elements contained in the composite catalysts. Temperature-programmed reduction (TPR, Quantachrome-Autosorb-iQC-TPX, Florida, FL, USA) was used to detect the redox capacity of the catalysts. the structure of samples was characterized with a X-ray diffraction (XRD, 6100, Shimadzu Corporation, Tokyo, Japan), the scanning range is 20–80°, scanning rate is 6°/min. The degradation of MB and MO was monitored by measuring the absorbance in real time with a UV-*vis* spectrophotometer (UV-*vis*, DS-11, DeNovix Inc, Wilmington, DE, USA). The concentrations of MB and MO were determined based on the constructed calibration curves at maximum absorption wavelength (λ_{max} = 665 nm and λ_{max} = 465 nm, respectively). A pH meter (PB-10, Sartorius Instrument System Co., Ltd., Göttingen, Germany) was employed to check the pH values of solutions.

3.4. Decolorization

In order to eliminate the influence of external factors on the experiment, all the decolorizations were carried out in a darkness clean laboratory at ambient temperature, and each experiment was completed three times at least. The UV-*vis* absorbance readings were taken using the spectrophotometer at λ_{max} = 665 nm for MB and λ_{max} = 465 nm for MO. In the decolorization experiments, a quantitative composite nano-PAA-$CuCl_2$ catalyst was added to a 10 mL dye solution with 50 mg/L concentration. After reaching the equilibrium, about 5 mL H_2O_2 was added to drive the decolorization progress. During the degradation, a little intermixture was taken every 2 min and immediately centrifuged, and then measured and analyzed with the UV-*vis* spectrophotometer. To test the stability and recyclability of nano-PAA-$CuCl_2$ catalyst, after the applied catalyst being filtered, washed and dried, the next identical decolorization cycle was repeated. The degradation

degrees of MB and MO were characterized by the parameter (C/C_0), which defined as the ratio of the post-degradation concentration (C) to the pre-degradation concentration (C_0).

4. Conclusions

A new composite of nano-PAA-CuCl$_2$ nanostructure film, a network porous CuCl$_2$ nanoflake film grown on the upper surface of nano-PAA substrate, was fabricated by self-assembly approach and used as a catalyst for degradation of organic pollutants such as MB and MO solutions in the Fenton-like reaction. The characteristics of composition, surface morphology and space structure of nano-PAA-CuCl$_2$ were systematically determined with various methods, e.g., EDS, XPS, HR-TEM, XRD and FE-SEM. The new composite nano-PAA-CuCl$_2$ had controllable three-dimensional network porous nanostructures, and stable physical and chemical properties.

The degradation of the MB and MO solution with the nano-PAA-CuCl$_2$ composite in the Fenton-like reaction was monitored in real time, and various factors affecting the catalytic reaction, for example, the initial pH, H$_2$O$_2$ concentration, catalyst morphology and working temperature, were investigated in detail. Under the optimum conditions, i.e., with 8×10^{-4} mol/L nano-PAA-CuCl$_2$ catalyst, at 30 °C and appropriate H$_2$O$_2$ 18 mM reagent, MB solution and MO solution could be completely degradation. And composite nano-PAA-CuCl$_2$ had good recyclability and stability. In particular, the MB solutions could be degraded completely (~100%) for three times, and the MO solution had been almost completely done for two times (~95%). Moreover, when the composite nano-PAA-CuCl$_2$ catalyst was continuously used repeatedly, even in the fifth time, it still maintained a high degradation rate (about 90% for MB and ~80% for MO). The main reasons can be attributed to the new nanoporous materials have a larger specific surface area and more active sites, which can greatly improve the removal efficiency of pollutants and realize deep removal of organic pollutants in wastewater. Besides improving the catalytic activity, the nano-PAA-CuCl$_2$ catalyst broadened the effective pH range of the reaction solution; the Fenton-like reaction was carried out without an acidification process which is another important advantage. In addition, the catalytic degradation mechanism of MB and MO by the nano-PAA-CuCl$_2$/H$_2$O$_2$ system conformed to the pseudo-first-order equation, based on the experimental data of the BCA and the H$_2$-TPR and theoretical analysis.

The network nano-PAA-CuCl$_2$ composite and preparation technology as well as its application in the Fenton-like reaction have excellent advantages, such as easy separation and recovery, higher degradation rate, lower H$_2$O$_2$ dosage, wider working pH range and multiple reusability, which will provide an effective alternative way with practical application significance for wastewater treatment.

References

1. Cai, Z.; Sun, Y.; Liude, W.; Pan, F.; Sun, P.; Fu, J. An overview of nanomaterials applied for removing dyes from wastewater. *Environ. Sci. Pollut. Res.* **2017**, *24*, 15882–15904. [CrossRef]
2. Pandey, S. A comprehensive review on recent developments in bentonite-based materials used as adsorbents for wastewater treatment. *J. Mol. Liq.* **2017**, *241*, 1091–1113. [CrossRef]
3. Fu, J.; Kyzas, G.Z. Wet air oxidation for the decolorization of dye wastewater: An overview of the last two decades. *Chin. J. Catal.* **2014**, *35*, 1–7. [CrossRef]
4. Zhang, J.; Li, F.; Sun, X.-Y. Rapid and selective adsorption of cationic dyes by a unique metal-organic framework with decorated pore surface. *Appl. Surf. Sci.* **2018**, *440*, 1219–1226. [CrossRef]

5. Bhatnagar, A.; Kaczala, F.; Hogland, W.; Marques, M.; Paraskeva, C.A.; Papadakis, V.G.; Sillanpää, M. Valorization of solid waste products from olive oil industry as potential adsorbents for water pollution control—A review. *Environ. Sci. Pollut. Res.* **2014**, *21*, 268–298. [CrossRef] [PubMed]

6. Yagub, M.T.; Sen, T.K.; Afroze, S.; Ang, H. Dye and its removal from aqueous solution by adsorption: A review. *Adv. Colloid Interface Sci.* **2014**, *209*, 172–184. [CrossRef] [PubMed]

7. Feng, L.; Van Hullebusch, E.D.; Rodrigo, M.A.; Esposito, G.; Oturan, M.A. Removal of residual anti-inflammatory and analgesic pharmaceuticals from aqueous systems by electrochemical advanced oxidation processes. A review. *Chem. Eng. J.* **2013**, *228*, 944–964. [CrossRef]

8. Naumczyk, J.; Bogacki, J.; Marcinowski, P.; Kowalik, P. Cosmetic wastewater treatment by coagulation and advanced oxidation processes. *Environ. Technol.* **2013**, *35*, 541–548. [CrossRef]

9. Antonopoulou, M.; Evgenidou, E.; Lambropoulou, D.; Konstantinou, I.K. A review on advanced oxidation processes for the removal of taste and odor compounds from aqueous media. *Water Res.* **2014**, *53*, 215–234. [CrossRef]

10. Oturan, M.A.; Aaron, J.-J. Advanced Oxidation Processes in Water/Wastewater Treatment: Principles and Applications. A Review. *Crit. Rev. Environ. Sci. Technol.* **2014**, *44*, 2577–2641. [CrossRef]

11. Mirzaei, A.; Chen, Z.; Haghighat, F.; Yerushalmi, L. Removal of pharmaceuticals from water by homo/heterogonous Fenton-type processes—A review. *Chemosphere* **2017**, *174*, 665–688. [CrossRef] [PubMed]

12. Navalón, S.; De Miguel, M.; Martin, R.; Alvaro, M.; Garcia, H. Enhancement of the Catalytic Activity of Supported Gold Nanoparticles for the Fenton Reaction by Light. *J. Am. Chem. Soc.* **2011**, *133*, 2218–2226. [CrossRef] [PubMed]

13. Martins, R.C.; Silva, A.M.T.; Castro-Silva, S.; Garção-Nunes, P.; Quinta-Ferreira, R.M. Advanced oxidation processes for treatment of effluents from a detergent industry. *Environ. Technol.* **2011**, *32*, 1031–1041. [CrossRef] [PubMed]

14. Sun, S.-P.; Zeng, X.; Lemley, A.T. Nano-magnetite catalyzed heterogeneous Fenton-like degradation of emerging contaminants carbamazepine and ibuprofen in aqueous suspensions and montmorillonite clay slurries at neutral pH. *J. Mol. Catal. A Chem.* **2013**, *371*, 94–103. [CrossRef]

15. Sun, S.-P.; Zeng, X.; Li, C.; Lemley, A.T. Enhanced heterogeneous and homogeneous Fenton-like degradation of carbamazepine by nano-Fe_3O_4/H_2O_2 with nitrilotriacetic acid. *Chem. Eng. J.* **2014**, *244*, 44–49. [CrossRef]

16. Zhang, Y.; Liu, C.; Xu, B.; Qi, F.; Chu, W. Degradation of benzotriazole by a novel Fenton-like reaction with mesoporous Cu/MnO_2: Combination of adsorption and catalysis oxidation. *Appl. Catal. B Environ.* **2016**, *199*, 447–457. [CrossRef]

17. Zhao, W.; Liang, C.; Wang, B.; Xing, S. Enhanced Photocatalytic and Fenton-Like Performance of CuO_x Decorated $ZnFe_2O_4$. *ACS Appl. Mater. Interfaces* **2017**, *9*, 41927–41936. [CrossRef]

18. Lyu, L.; Zhang, L.; Hu, C. Enhanced Fenton-like degradation of pharmaceuticals over framework copper species in copper-doped mesoporous silica microspheres. *Chem. Eng. J.* **2015**, *274*, 298–306. [CrossRef]

19. Li, Z.; Lyu, J.; Ge, M. Synthesis of magnetic Cu/$CuFe_2O_4$ nanocomposite as a highly efficient Fenton-like catalyst for methylene blue degradation. *J. Mater. Sci.* **2018**, *53*, 15081–15095. [CrossRef]

20. Verma, P.; Shah, V.; Baldrian, P.; Gabriel, J.; Stopka, P.; Trnka, T.; Nerud, F. Decolorization of synthetic dyes using a copper complex with glucaric acid. *Chemosphere* **2004**, *54*, 291–295. [CrossRef]

21. Nichela, D.A.; Berkovic, A.M.; Costante, M.R.; Juliarena, M.P.; Einschlag, F.S.G. Nitrobenzene degradation in Fenton-like systems using Cu(II) as catalyst. Comparison between Cu(II)- and Fe(III)-based systems. *Chem. Eng. J.* **2013**, *228*, 1148–1157. [CrossRef]

22. Li, J.-M.; Meng, X.; Hu, C.-W.; Du, J.; Zeng, X.-C. Oxidation of 4-chlorophenol catalyzed by Cu(II) complexes under mild conditions: Kinetics and mechanism. *J. Mol. Catal. A Chem.* **2009**, *299*, 102–107. [CrossRef]

23. Jain, A.; Balasubramanian, R.; Srinivasan, M. Production of high surface area mesoporous activated carbons from waste biomass using hydrogen peroxide-mediated hydrothermal treatment for adsorption applications. *Chem. Eng. J.* **2015**, *273*, 622–629. [CrossRef]

24. Lee, Y.-C.; Dutta, S.; Wu, K.C.-W. Integrated, Cascading Enzyme-/Chemocatalytic Cellulose Conversion using Catalysts based on Mesoporous Silica Nanoparticles. *ChemSusChem* **2014**, *7*, 3181. [CrossRef]

25. Gao, S.; Han, Y.; Fan, M.; Li, Z.; Ge, K.; Liang, X.J.; Zhang, J. Metal-organic framework-based nanocatalytic medicine for chemodynamic therapy. *Sci. China Mater.* **2020**, *63*, 2429–2434. [CrossRef]

26. Araoyinbo, A.O.; Derman, M.N.; Rahmat, A.; Ahmad, K.R. Organic Dye Degradation with TiO_2 Catalyst/AAO Template in the Presence of H_2O_2. *Adv. Mater. Res.* **2013**, *795*, 649–653. [CrossRef]

27. Cheng, Y.; Wang, K.; Zhou, Y.; Sun, D.; Zhang, C.; Zhao, W.; Bai, J. Enhanced degradation effect of nano-PAA–$CuCl_2$ with controllable 3D structure as heterogeneous Fenton-like catalyst over a wide pH range. *J. Mater. Sci.* **2019**, *54*, 7850–7866. [CrossRef]

28. Ramirez, J.H.; Maldonado-Hódar, F.J.; Pérez-Cadenas, A.F.; Moreno-Castilla, C.; Costa, C.A.; Madeira, L.M. Azo-dye Orange II degradation by heterogeneous Fenton-like reaction using carbon-Fe catalysts. *Appl. Catal. B Environ.* **2007**, *75*, 312–323. [CrossRef]

29. Wang, X.; Pan, Y.; Zhu, Z.; Wu, J. Efficient degradation of rhodamine B using Fe-based metallic glass catalyst by Fenton-like process. *Chemosphere* **2014**, *117*, 638–643. [CrossRef]

30. Lee, H.-J.; Lee, H.; Lee, C. Degradation of diclofenac and carbamazepine by the copper(II)-catalyzed dark and photo-assisted Fenton-like systems. *Chem. Eng. J.* **2014**, *245*, 258–264. [CrossRef]

31. Torrades, F.; García-Montaño, J. Using central composite experimental design to optimize the degradation of real dye wastewater by Fenton and photo-Fenton reactions. *Dyes Pigments* **2014**, *100*, 184–189. [CrossRef]

32. Wiechelman, K.J.; Braun, R.D.; Fitzpatrick, J.D. Investigation of the bicinchoninic acid protein assay: Identification of the groups responsible for color formation. *Anal. Biochem.* **1988**, *175*, 231–237. [CrossRef]

33. Jie, L.; Xueju, L.; Zhou, G.; Zhen, K.; Zhang, W.; Cheng, T. Effect of kcl on cucl/γ-alo catalyst for oxychlorination of ethane. *React. Kinet. Catal. Lett.* **2006**, *88*, 315–324.

34. Rouco, A. TPR study of Al_2O_3- and SiO_2-supported $CuCl_2$ catalysts. *Appl. Catal. A Gen.* **1994**, *117*, 139–149. [CrossRef]

35. Perez-Benito, J.F. Reaction pathways in the decomposition of hydrogen peroxide catalyzed by copper(II). *J. Inorg. Biochem.* **2004**, *98*, 430–438. [CrossRef]

36. González-Dávila, M.; Santana-Casiano, J.; González, A.; Pérez, N.; Millero, F. Oxidation of copper(I) in seawater at nanomolar levels. *Mar. Chem.* **2009**, *115*, 118–124. [CrossRef]

37. Wu, J.; Wang, K.; Zhou, Y.; Wang, S.; Zhang, C.; Wang, G.; Bai, J. Synthesis and photoluminescence enhancement of nano-PAA-$ZnCl_2$ with controllable dimension and morphology. *Appl. Surf. Sci.* **2016**, *390*, 122–130. [CrossRef]

38. Hanqing, B.; Kaige, W.; Yang, J.; Aizi, J.; Jintao, B.; Changzhi, G. Real-time Study of Mechanism of 3D Pore-Widening for Nano-Porous Anodic Alumina Based on a Multilayer Structure Theory. *Rare Metal Mater. Eng.* **2017**, *46*, 1536–1542. [CrossRef]

39. Wang, K.; Wang, K.; Wang, S.; Ren, J.; Bai, X.; Bai, J. SERS activity with tenfold detection limit optimization on a type of nanoporous AAO-based complex multilayer substrate. *Nanoscale* **2016**, *8*, 5920–5927. [CrossRef]